J Mater Sci: Mater Electron
DOI 10.1007/s10854-011-0490-y

Fabrication of highly *c*-axis textured ZnO thin films piezoelectric transducers by RF sputtering

Min-Chun Pan · Tzon-Han Wu · Tuan-Anh Bui · Wen-Ching Shih

Received: 29 May 2011 / Accepted: 4 August 2011

Abstract The influence of fabrication parameters on ZnO film properties has been analyzed through conducting several experiment processes to develop an appropriate deposition condition for obtaining highly *c*-axis textured films. A transducer with the structure of Al/ZnO/Al/Si was fabricated at low deposition rate and under a temperature of 380 °C in a mixture of gases $Ar:O_2 = 1:3$, and RF power of 178 W. Pt/Ti was employed as the bottom electrode of the transducer fabricated in a suitable substrate temperature, which starts increasing at 380 °C with an increment of 20 °C for each 2 h stage of the deposition. Highly *c*-axis textured ZnO films have been successfully deposited on $Pt/Ti/SiO_2/Si$ substrate under feasible conditions, including RF power of 178 W, substrate temperature of 380 °C, deposition pressure of 1.3 Pa and $Ar:O_2$ gas flow ratio of 50%. These conditions have been proposed and confirmed through investigating the influences of the sputtering parameters, such as substrate temperature, RF power and $Ar:O_2$ gas flow ratio, on the properties of ZnO films.

M.-C. Pan · T.-H. Wu · T.-A. Bui
Department of Mechanical Engineering, National Central University, No. 300, Jhongda Rd., Jhongli City, Taoyuan County 320, Taiwan, ROC

M.-C. Pan
Graduate Institute of Biomedical Engineering, National Central University, No. 300, Jhongda Rd., Jhongli City, Taoyuan County 320, Taiwan, ROC

W.-C. Shih (✉)
Graduate Institute in Electro-Optical Engineering, Tatung University, No. 40, Sec. 3, Chungshan North Road, Taipei 104, Taiwan, ROC
e-mail: wcshih@ttu.edu.tw

1 Introduction

Ultrasonic ejector [1–3] is capable of ejecting small droplets of controlled diameter from a free liquid surface by focusing high-frequency acoustic wave without using a nozzle; and therefore, it is favorable in the fabrication of print-heads. The key elements of an ultrasonic ejector include a piezoelectric transducer and an ultrasonic focusing lens. Piezoelectric transducer has been used to generate ultrasound which will be focused by an ultrasonic focusing lens for the purpose of droplet ejection. ZnO exhibits that it is a promising material which is most studied and widely applied in piezoelectric transducer due to good piezoelectric properties and high electro-mechanical coupling coefficient [4]. It is, therefore, a potential material for producing transducers and sensors such as communication applications using ultra-high frequency surface acoustic wave (SAW) devices [4] or bulk acoustic wave resonators [5]. In order to enhance high-quality ZnO films, several deposition techniques have been employed and developed such as sputtering [4, 6, 7], metal–organic chemical-vapor deposition [8], pulsed laser deposition [9] and molecular beam epitaxy [10]. Properties of ZnO films strongly depend on the deposition conditions such as bottom electrode materials [11–13] and other fabrication parameters including RF power [12, 13], deposition pressure, substrate temperature [13, 14], and deposition gas composition ($Ar:O_2$) [11, 13–15].

RF magnetron sputtering method, which offers a simple process and low equipment cost, was employed in our experiments in order to develop a feasible fabrication of ZnO thick films. The effects of deposition conditions such as substrate temperature, RF power and $Ar:O_2$ gas flow ratio, on the growth of ZnO films were investigated in detail. The ZnO films were sputtered on various substrates,

Published online: 14 August 2011

including Al/Si and Pt/Ti/SiO_2/Si. The ZnO thin film piezoelectric transducers were fabricated and their responses were measured through the impedance analysis.

2 Piezoelectric transducer

Piezoelectric transducer is considered as a key component of acoustic inkjet print-heads, which generates ultrasonic waves by inverse piezoelectric effect with an input of high frequency signal. Efficient generation of ultrasonic waves is important to minimize the required energy of RF signals, thereby reducing the power of the print-head. ZnO thin film growth and processing approaches are crucial for fabricating various ultrasonic frequency transducers with a uniform response. Piezoelectric ZnO film provides a relatively high electromechanical coupling coefficient and reasonable compatibility with integrated circuit processing techniques. Moreover, no adhesion layer is required for bonding the transducer layer to the substrate or electrode layer.

In an air or water media, most of the wave energy will be reflected at the boundaries of the piezoelectric film. The sound waves which are unexpectedly reflected must affect the sound convergence at the focal area and ejection performance. This problem is solved when the transducer is attached a backing material on the back side with its acoustic impedance close to that of the piezoelectric film. Backing layer makes no energy left to be reflected from the end of backing and affects the sound energy convergence [16]. Furthermore, backing layer prevents the piezoelectric array from over-vibrating so that the array must stop working once exciting voltage is at the rest of driving signals [17].

Shown in Fig. 1, is a scheme of a piezoelectric transducer. The mechanical force can be considered as the analog of the electrical voltage and the particle velocity as the analog of the electrical current, the electrical input impedance of a transducer can be expressed as [18]

$$Z_{in} = \frac{V}{I} = \frac{1}{j\omega C_0} \left[1 + \frac{k_e^2}{kd} \cdot \frac{j(Z_1 + Z_2)Z_a \sin kd - 2Z_a^2(1 - \cos kd)}{(Z_a^2 + Z_1 Z_2)\sin kd - j(Z_1 + Z_2)Z_a \cos kd}\right] \quad (1)$$

Where Z_a is the acoustic impedance of the piezoelectric film, Z_1 and Z_2 are the acoustic impedance of the top and bottom sides of the piezoelectric film, respectively. Since the electrodes of the transducer are very thin, Z_1 and Z_2 can be neglected. Then the RF input impedance of the transducer is

$$Z_{in} = \frac{V}{I} = \frac{1}{j\omega C_0}\left[1 - k_e^2 \frac{\tan(kd/2)}{kd/2}\right] \quad (2)$$

where $C_0 = \frac{\varepsilon^S A}{d}$ and $k_e^2 = \frac{e^2}{c^E \varepsilon^S}$ are the static capacitor and electro-mechanical coupling constant, respectively [19]; k is the acoustic wave number; d is the thickness of piezoelectric layer.

Substituting the parameters of ZnO piezoelectric material to Eq. 2, and using Matlab software to simulate the impedance at various thicknesses d of ZnO films as shown in Fig. 2. The relationship between thickness and corresponding resonant frequency was obtained and listed in Table 1. That relation can be expressed by

$$d \times f_r = 3070\,(\mu\text{mMHz}) \quad (3)$$

where f_r is the resonant frequency of piezoelectric transducer.

3 Fabrication of ZnO piezoelectric transducer

In this section, we present the fabrication process of ZnO transducers with a sandwich type including top electrode, ZnO piezoelectric film and bottom electrode. To investigate the effects of various deposition conditions on the properties of ZnO films, some fabrication trials were performed to find the most appropriate.

In the first experiment, the Al bottom electrode was deposited using evaporator at room temperature and deposition pressure of 2.5×10^{-5} mbar. The ZnO film was subsequently sputtered at 380 °C in a mixture of gases $Ar:O_2 = 1:3$, and a RF power of 178 W. The Al upper electrode is finally deposited by evaporator in the same manner with bottom electrode to complete the fabrication of transducer. The fabrication process of the piezoelectric transducer was described as shown in Fig. 3.

Other experimental process, we used Pt/Ti layers as the bottom electrode. Since our previous experiences when using Al as the bottom electrode, the orientation of ZnO thin film is still disordered because of its amorphous layer around the ZnO/Al interface. Therefore, Pt/Ti was considered with purpose of obtaining a better orientation of ZnO thin film. Actually, Pt is hardly oxidized and Ti thin film is used as a buffer layer of Pt bottom electrode on silicon wafer to improve the adhesive durability between bottom electrode and substrate. Hence, a thin layer of SiO_2 was created on a cleaned-silicon wafer, and 20 nm thickness of Ti film was subsequently deposited. Pt was used as the bottom electrode with thickness of 150 nm in the fabrication. The transducer structure, therefore, is Al(100 nm)/ZnO/Pt(150 nm)/Ti(20 nm)/SiO_2(150 nm)/Si. In order to analyze the influence of sputtering conditions such as substrate temperature, RF power and sputtering gas composition on the growth of ZnO films to determine the most feasible deposition conditions, we tried to deposit ZnO thin

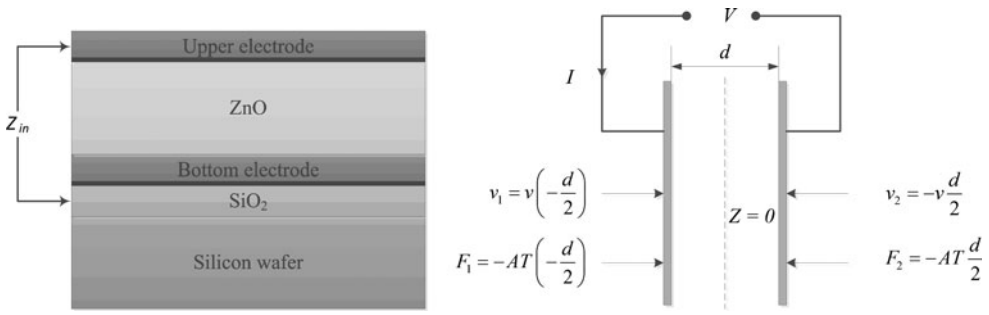

Fig. 1 Schematic diagram of piezoelectric transducer

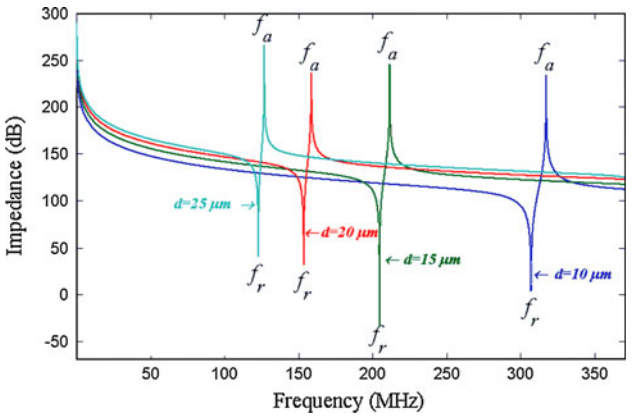

Fig. 2 Simulated impedances at various thicknesses of ZnO films

Table 1 ZnO thickness and corresponding resonant frequency

d (μm)	10	15	20	25	30	35
f_r (MHz)	307.05	204.7	153.52	122.82	102.35	87.73

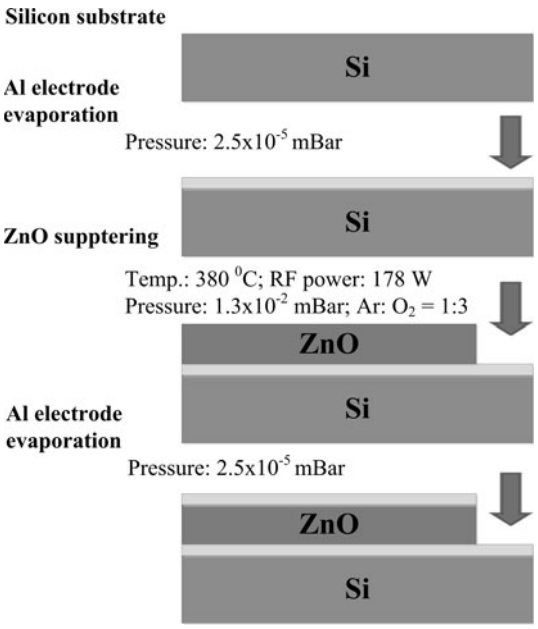

Fig. 3 Fabrication process of piezoelectric transducer

films in several set of sputtering parameters as follows. Firstly, the substrate temperature was varied from 380 to 500 °C while other parameters need to be determined in advance including a mixture of gases Ar:O_2 = 50:50, and a RF power of 178 W to find a suitable substrate temperature that improves the *c*-axis orientation intensity. Secondly, since results of our previous experiments, the most reasonable substrate temperature for the sputtering process of ZnO films is 380 °C which was confirmed. Here, 1.3 Pa is the deposition pressure kept fixed while varying other factors. Remain the gas flow ratio of Ar:O_2 in 1:1, and sputter ZnO films under the RF powers of 120, 150 and 178 W, respectively, in order to consider the effect of RF power on the growth of ZnO films. Similarly, various compositions, 20, 40 and 50%, of oxygen of the sputtering gas were also employed to consider the influence of those compositions on *c*-axis orientation of ZnO films.

The distance between a 4 inch ZnO target and substrate was kept fixed at 45 mm for all our experiments. After the confirmation of X-ray diffraction (XRD) patterns, Al evaporation and patterning was performed to shape the top electrode of the transducer. The thickness of the ZnO film was measured by Dektak^{3}ST α-step surface profiler. The XRD pattern of ZnO films was measured by Siemens D5000 diffractometer. Finally, the transducer performance was tested through the impedance analysis by using the Agilent 4395A instrument.

4 Results and discussion

The XRD is an important examining instrument for determining the structure characteristics of materials, such as orientation, crystalline structure, lattice parameters, lateral displacement, defect density and drain size. To consider whether the crystalline structure is fine or not, the diffraction intensity of the ZnO(002) peak observed is relatively strong in comparison to that of the other peaks. In general, the diffraction intensity of the ZnO(002) peak must be about five times higher than that of other peaks.

In the first experiment, the XRD shown in Fig. 4, the diffraction peaks of the ZnO film has strong intensity in

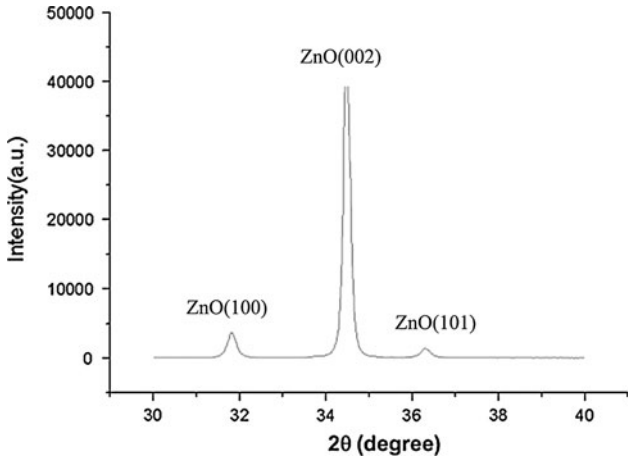

Fig. 4 X-ray diffraction pattern for ZnO film with deposition time of 4 h

c-axis orientation at a diffraction angle of 34.4° which is close to the corresponding value for ZnO bulk (JCPDS No. 36-1451). Apparently, it is observed in Fig. 4 that the diffraction intensity of the ZnO(002) peak is more than five times higher than those of the other peaks. That means the piezoelectric characteristics must be clear. On the other hand, the average thickness about 3 μm is obtained in sputtering time of 4 h, thus we may suppose that the average sputtering rate is 0.75 μm/h. This is still a drawback of sputtering process of thick ZnO films that needs to be improved.

In the second experiment, we expect to find an appropriate substrate temperature to obtain a high *c*-axis orientation of ZnO films. Indeed, in this experiment, ZnO films were deposited at substrate temperature of 380, 500, 600, and 800 °C for that purpose. Actually, the deposition period was divided into four stages, every stage lasts 2 h with the same temperature as mentioned, and an idle time between each two deposition stages is 2 h. However, the ZnO films were flaked off the wafer at temperature of 800 °C. That is probably because of the different thermal expansion coefficient between the ZnO film and substrate in the idle stage. Therefore, Fig. 5 presents the XRD patterns of ZnO films deposited at substrate temperature of 380, 500, and 600 °C, respectively. Besides, it can be seen that the intensity of the ZnO(002) peak increases and subsequently decreases along with deposition time, and the highest ZnO(002) peak appears after the second 2-h stages for all substrate temperature. That means, the intensity of ZnO(002) peak rises as ZnO film thickness increases due to a larger size of polycrystallinity in the second stage. However, the intensity decreases after a certain thickness of ZnO film. It is presumed that, after the polycrystallinity becomes larger as the ZnO film thickness increases in the second stage, it gradually decreases and is main cause of

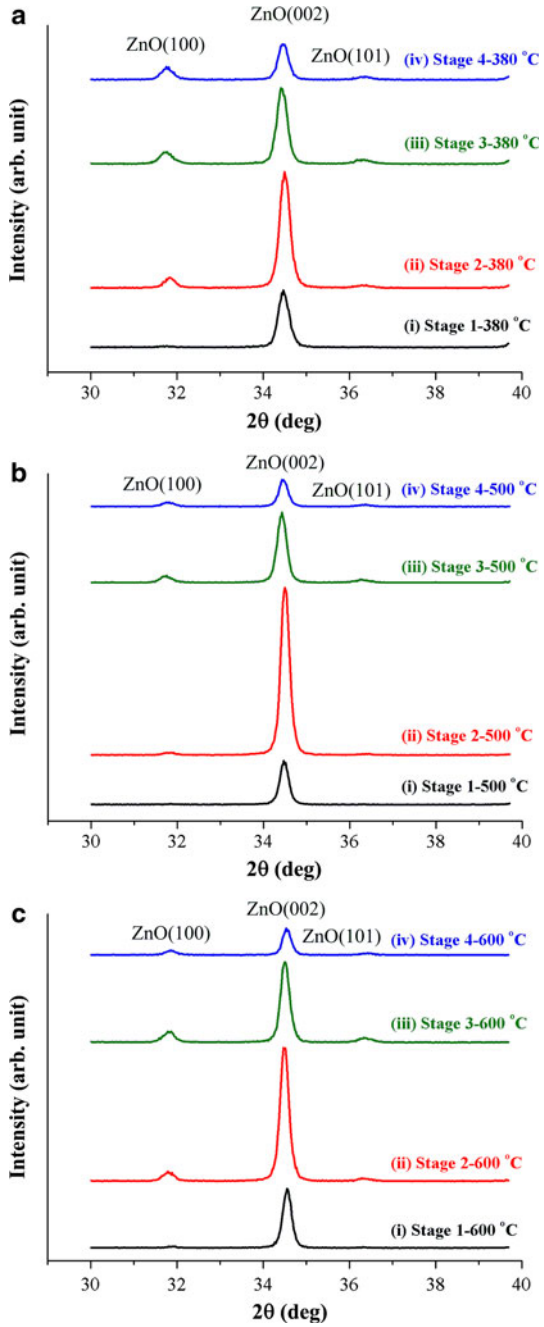

Fig. 5 XRD patterns of the ZnO films deposited at different substrate temperatures of **a** 380 °C, **b** 500 °C, and **c** 600 °C

reduction of the intensity of ZnO(002) peak after the second 2-h stages.

As known that, a stable substrate temperature in each stage of ZnO film deposition process will not increase the diffraction intensity of the ZnO(002) peak when the deposition time was increased. Hence, we consider three cases of temperature change when depositing the ZnO films in this experiment. In which, 2 h are still spent for every stage of the deposition. The change of the temperature was varied in three cases, which include increasing the substrate

temperature at 380 °C with an increment of 20 and 40 °C for each stage, and lowering the substrate temperature at 440 °C with a decrement of 20 °C for each stage, respectively.

Figure 6 illustrates the XRD patterns of the ZnO films deposited at three cases of temperature change as above-mentioned. Shown in Fig. 6c, the diffraction intensity of the ZnO(002) peak becomes increasingly weaker in every stage. The same problem is still revealed in Fig. 6b. That is, in comparison with the diffraction intensity of the other orientation peak, the ZnO(002) peak does not become relatively stronger. Besides, Fig. 6a is clearly observed that the diffraction intensity of the ZnO(002) peak becomes relatively stronger as compared with other orientation peak when the deposition time was increased. Especially, in stage 4, the diffraction intensity of the ZnO(002) peak is over 22 times higher than that of the second-highest peak. Moreover, the FWHM value of ZnO(002) peak is smaller in every stage. The results shown in Fig. 6a and b have a good agreement with the conclusion of increasing the deposition rate and polycrystallinity of ZnO film when the substrate temperature was increased [20, 21]. That means the *c*-axis orientation of crystallite increases as the substrate temperature was increased and vice versa. However, the results illustrated in Fig. 6c and stage 2 in Fig. 6b are not right for the consideration which is mentioned above, because the *c*-axis preferred orientation of ZnO films depends on many factors in the fabrication process such as preferential nucleation, preferential crystallization, sticking, etc. [20]. Therefore, ZnO films deposited adopts the substrate temperature of the first case to execute following characteristics measurements.

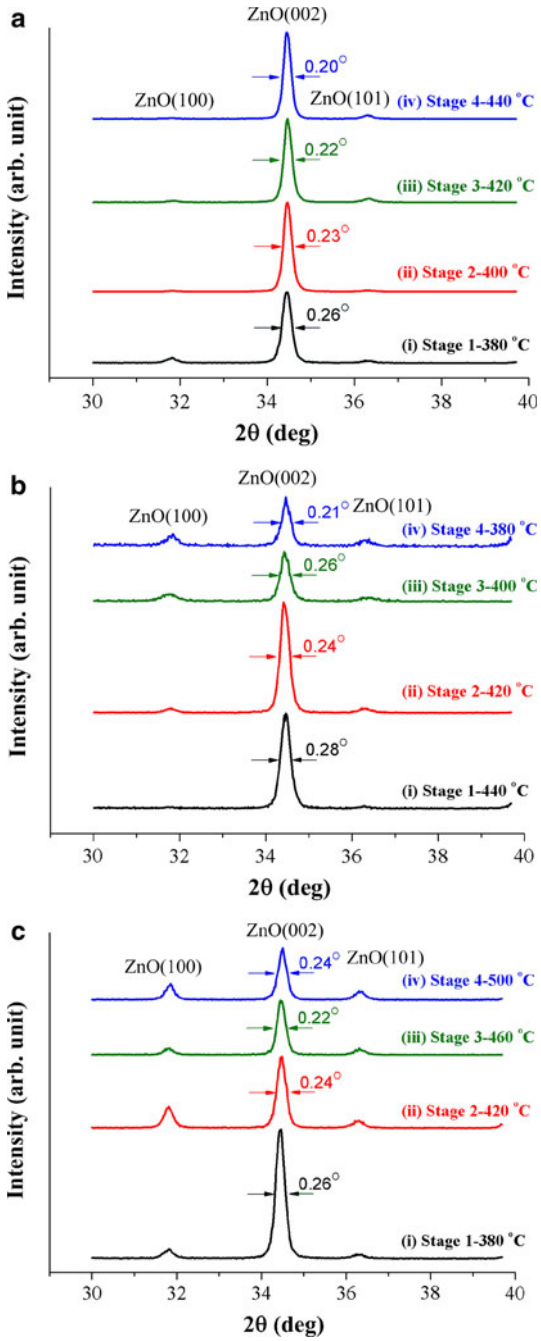

Fig. 6 XRD patterns of the ZnO films deposited at various substrate temperature changing cases: **a** 380 → 400 → 420 → 440 °C, **b** 440 → 420 → 400 → 380 °C, and **c** 380 → 420 → 460 → 500 °C

Basing on the XRD results of ZnO films deposited under the RF powers of 120, 150 and 178 W, respectively, to determine the most appropriate power. The XRD patterns of these ZnO films (illustrated in Fig. 7) showed the highest diffraction intensity in *c*-axis orientation with a RF power of 178 W. That is, high RF power leads to high energy of particles to impact on the film surface, increase atom intensity and tend towards fine columnar grain structure [22, 23], this means a preferred ZnO film is obtained. Similarly, the most appropriate gas flow ratio of 50% for the *c*-axis ZnO(002) orientation of ZnO film growth was determined, that is demonstrated through the XRD results shown in Fig. 8. That is, more O_2 gas reduces the deposition rate because of a higher collision between Ar and O atoms [22], this may cause a reduction of energy of particles, reduce the adhesion of particles on the film surface and effect on the *c*-axis crystallographic direction.

After determining the most appropriate sputtering conditions for our purpose including substrate temperature, RF power and gas flow ratio of Ar:O_2, different thicknesses of ZnO films were deposited to produce several piezoelectric transducers working at different resonant frequencies. The (002) orientation of ZnO films which is one of the most important factors helping determine an appropriate set of deposition parameters for the piezoelectric transducer of ultrasonic ejector application, was considered first. And then, another parameter of ZnO thin films needs to be characterized is the impedance measurement of ZnO films. For this purpose, a top electrode was deposited on the film

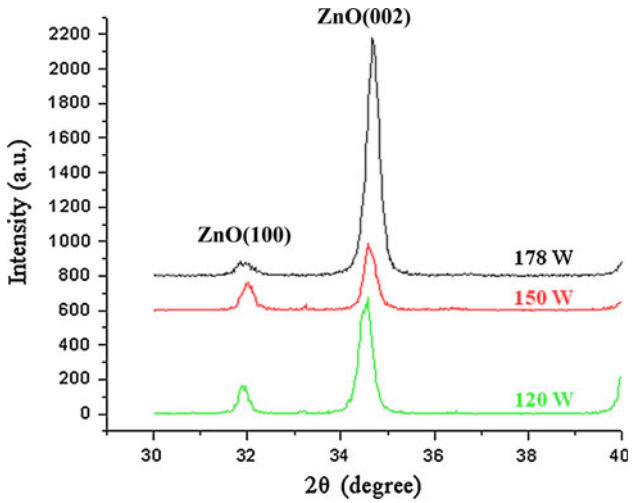

Fig. 7 XRD patterns of ZnO films fabricated under the RF powers of 120, 150 and 178 W, respectively

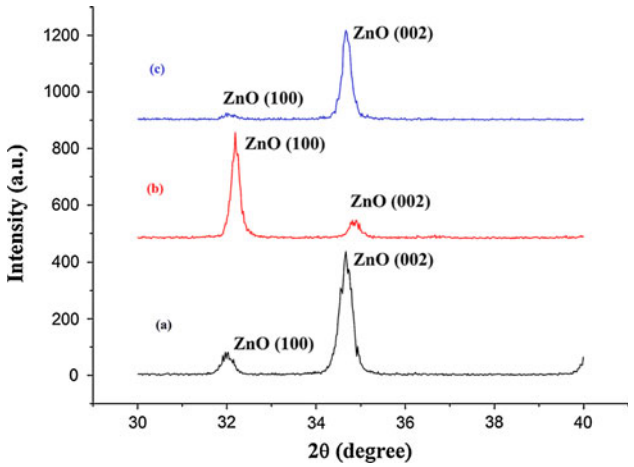

Fig. 8 XRD patterns of ZnO films fabricated under **a** 20%, **b** 40% and **c** 50%, of oxygen of the sputtering gas, respectively

to complete the ZnO transducer structure and an impedance measurement was set up. The measurement was performed by using the Agilent 4395A impedance analyzer to observe the resonant frequency. To evaluate the relation between film thickness, impedance and resonant frequency, it is necessary to take the measurement with different thicknesses of ZnO film of the transducer. Thicknesses of deposited ZnO films are 15.28, 20.92, and 26.72 μm corresponding to the deposition time of 8, 10, and 12 h, respectively. The impedance of different thicknesses as mentioned above were measured and the results are shown in Fig. 9.

Further, the resonance and anti-resonance frequencies of simulation and measurement are listed in Table 2. The measurement results indicate that the frequencies of ZnO films were decreased when their thicknesses were increased. In comparison with the simulated values, the

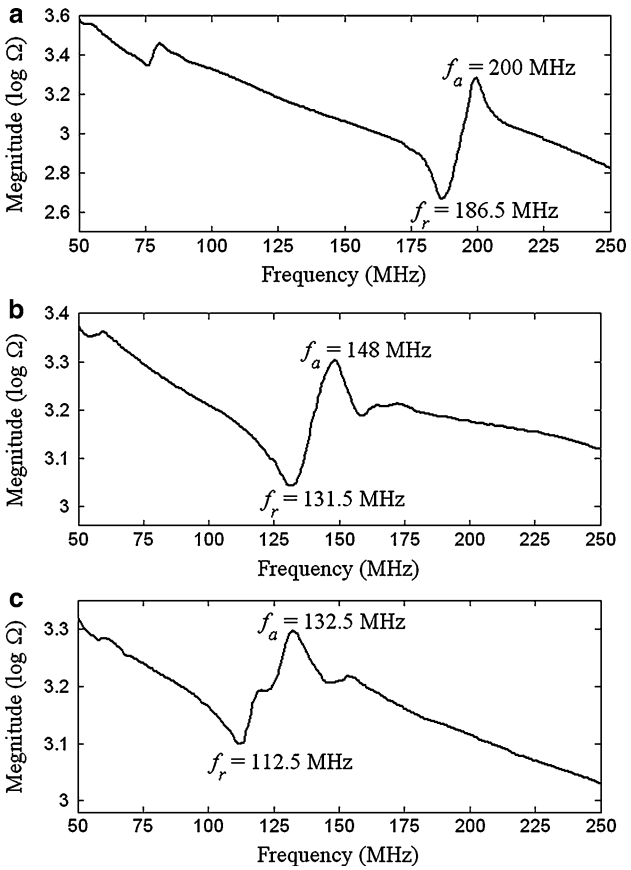

Fig. 9 Impedances of ZnO films deposited with different thicknesses: **a** 15.28 μm, **b** 20.92 μm, and **c** 26.72 μm

differences between these two results are about 7–10%. That can be explained the thicknesses of ZnO films are measured at the border the films. These thicknesses are thinner than those at the center of ZnO films. Hence, the measured resonance frequencies are lower than the values of simulation. Besides, this is presumably because the mass loading effects caused by the electrodes on ZnO film leading the actual resonant frequency becomes lower than the simulation result which is mentioned above. Further, the influences of other factors as room temperature, humidity, measured fixture, etc. on the results of measurement are also related. In addition, the fabrication of the ultrasonic focusing lens, which will be integrated with the piezoelectric transducer to produce an ultrasonic ejector, is carrying out and improving. A setup of experiment, which is to see the performance of that ultrasonic ejector, is under consideration.

5 Conclusions

ZnO films of the piezoelectric transducer for ultrasonic ejector application were deposited by RF magnetron

Table 2 Resonance frequencies of ZnO films for simulation and actual fabrication

Deposition time (h)	Thickness (μm)	Simulation (MHz)		Measurement (MHz)		Error (%)	
		f_r	f_a	f_r	f_a	f_r	f_a
8	15.28	200.95	207.64	186.5	200	7.19	3.68
10	20.92	146.77	151.66	131.5	148	10.41	2.41
12	25.34	121.17	125.21	112.5	132.5	7.16	5.83

sputtering and the influences of fabrication parameters on the properties of ZnO films have been investigated and discussed in detail through some experiment processes. The high *c*-axis orientation was observed in each experimental conditions, however, the drawback were also revealed and needed to be solved. A low deposition rate in the first experiment (Al/ZnO/Al/Si structure) is a trouble when sputtering a thick ZnO film for high frequency piezoelectric transducer. The structure of piezoelectric transducer Al/ZnO/Pt/Ti/SiO_2/Si, in the second experiment, offers advantages due to the properties of bottom electrode Pt/Ti are more stable than the conventional Al electrode. An appropriate substrate temperature is found to obtain high *c*-axis oriented ZnO films. That is, the temperature is started increasing at 380 °C with an increment of 20 °C for each 2 h stage of the deposition. A feasible fabrication of the piezoelectric transducer was proposed and justified through analyzing the influences of the deposition conditions on the properties of ZnO films. Under the conditions with the RF power of 178 W, the substrate temperature of 380 °C, deposition pressure of 1.3 Pa and the Ar:O_2 gas ratio of 50%, ZnO films were successfully deposited on Pt/Ti/SiO_2/Si substrate. These films show high *c*-axis orientations which is an essential condition that satisfies the requirements of piezoelectricity for a high-frequency piezoelectric transducer of an ultrasonic ejector application. Impedance analysis shows that the mass loading effects of the electrodes on the ZnO film are significant. That is, we need to consider these effects when designing and fabricating a device that works at a specific resonant frequency.

Acknowledgments This work was sponsored partly by the National Science Council of the Republic of China under contract No. NSC 99-2221-E-036-004 and partly by Tatung University under contract No. B99-O05-054. The authors greatly appreciated their financial support.

References

1. S.A. Elrod, B. Hadimioglu, B.T. Khuri-Yakub, E.G. Rawson, E. Richley, C.F. Quate, J. Appl. Phys. **65**, 3441 (1989)
2. H. Yu, Q. Zou, J.W. Kwon, E.S. Kim, J. Microelectromech. Syst. **16**, 445 (2007)
3. H. Fukumoto, J. Aizawa, H. Nakagawa, H. Narumiya, J. Imaging Sci. Technol. **44**, 398 (2000)
4. X.Y. Du, Y.Q. Fu, S.C. Tan, J.K. Luo, A.J. Flewitt, S. Maeng, S.H. Kim, Y.J. Choi, D.S. Lee, N.M. Park, J. Park, W.I. Milne, J. Phys. Conf. Ser. **76**, 012035 (2007)
5. K.W. Tay, P.H. Sung, Y.-C. Lin, T.J. Hung, J. Electroceram. **21**, 178 (2008)
6. Y. Lin, C. Hong, H. Chuang, Appl. Surf. Sci. **254**, 3780 (2008)
7. J.C. Zesch, B. Hadimioglu, B.T. Khuri-Yakub, M. Lim, R. Lujan, J. Ho, S. Akamine, D. Steinmetz, C.F. Quate, E.G. Rawson, Deposition of highly oriented low-stress ZnO films, in *IEEE Ultrasonics Symposium*, pp. 445–448 (1991)
8. Y. Cui, G. Du, Y. Zhang, H. Zhu, B. Zhang, J. Cryst. Growth **282**, 389 (2005)
9. B.J. Jin, S.H. Bae, S.Y. Lee, S. Im, Mater. Sci. Eng. B **71**, 301 (2000)
10. K. Iwata, P. Fons, S. Niki, A. Yamada, K. Matsubara, K. Nakahara, T. Tanabe, H. Takasu, J. Cryst. Growth **214–215**, 50 (2000)
11. R.C. Lin, Y.C. Chen, K.S. Kao, Appl. Phys. A Mater. Sci. Process. **89**, 475 (2007)
12. Y.H. Hsu, J. Lin, W.C. Tang, J. Mater. Sci. Mater. Electron. **19**, 653 (2008)
13. S. Chandra, V. Bhatt, R. Singh, Sadhana **34**, 543 (2009)
14. P.M. Martin, M.S. Good, J.W. Johnston, G.J. Posakony, L.J. Bond, S.L. Crawford, Thin Solid Films **379**, 253 (2000)
15. J. Golebiowski, J. Mater. Sci. **34**, 4661 (1999)
16. R. McKeighan, Design guidelines for medical ultrasonic arrays, in *Proceedings of SPIE International Symposium on Medical Imaging*, vol. 3341, p. 2 (1998)
17. S. Hirahara, T. Saito, H. Nagato, T. Itakura, S. Takayama, H. Nukada, S. Hattori, N.Y. Kudo, S. Saitoh, M. Sugiuchi, Y. Tokai, F. Murakami, H. Tanaka, C. Tanuma, M. Izumi, I. Amemiya, A. Nakamura, S. Shimizu, K. Okuwada, *Ink-Jet Recording Device Having an Ultrasonic Generating Element Array*, vol. 6045208, ed. by U.S. Patent (2000)
18. Z. Hao, P. Wei, K. Eun Sok, in *Frequency Control Symposium and Exposition*, High-frequency bulk acoustic resonant microbalances in liquid. Proceedings of the 2005 IEEE International (2005)
19. J.F. Rosenbaum, *Bulk Acoustic Wave Theory and Devices* (Artch House, Inc, Norwood, Massachusetts, 1988)
20. S. Singh, R.S. Srinivasa, S.S. Major, Thin Solid Films **515**, 8718 (2007)
21. Y. Suzaki, A. Kawaguchi, T. Murase, T. Yuji, T. Shikama, D.B. Shin, Y.K. Kim, Physica Status Solidi (C), **8**, 503 (2011)
22. S.H. Park, B.C. Seo, G. Yoon, H.D. Park, J. Vac. Sci. Technol. A, **18** 2432 (2000)
23. Y.C. Lin, C.R. Hong, H.A. Chuang, Appl. Surf. Sci. **254**, 3780 (2008)